nature communications

Article

https://doi.org/10.1038/s41467-025-58221-7

Metabolic constraint of human telomere length by nucleotide salvage efficiency

Received: 29 April 2024

Accepted: 14 March 2025

Published online: 27 March 2025

Check for updates

William Mannherz[1,2,3,4,5], Andrew Crompton[1,2,3,4], Noah Lampl[1,2,3] & Suneet Agarwal[1,2,3,4,5]

Human telomere length is tightly regulated and associated with diseases at either extreme, but how these bounds are established remains incompletely understood. Here, we developed a rapid cell-based telomere synthesis assay and found that nucleoside salvage bidirectionally constrains human telomere length. Metabolism of deoxyguanosine (dG) or guanosine via purine nucleoside phosphorylase (PNP) and hypoxanthine-guanine phosphoribosyltransferase to form guanine ribonucleotides strongly inhibited telomerase and shortened telomeres. Conversely, salvage of dG to its nucleotide forms via deoxycytidine kinase drove potent telomerase activation, the extent of which was controlled by the dNTPase SAMHD1. Circumventing limits on salvage by expressing *Drosophila melanogaster* deoxynucleoside kinase or augmenting dG metabolism using the PNP inhibitor ulodesine robustly lengthened telomeres in human cells, including those from patients with lethal telomere diseases. Our results provide an updated paradigm for telomere length control, wherein telomerase reverse transcriptase activity is actively and bidirectionally constrained by the availability of its dNTP substrates, in a manner that may be therapeutically actionable.

The ends of linear chromosomes are capped by hexameric repeat sequences termed telomeres, which are required for genomic integrity[1,2]. During genome replication, a terminal portion of telomeres is lost due to the inability of DNA polymerases to completely replicate linear chromosomes[3,4]. Loss of telomere sequence to a critically short length causes DNA damage signaling leading to cellular senescence and exit from the cell cycle[5]. In self-renewing cells, the telomerase reverse transcriptase (TERT) compensates for telomere shortening by synthesizing new 5′-GGTTAG-3′ repeats using the telomerase RNA template (TERC) and dNTP substrates[6–9]. In prevailing models of human telomere length regulation, the expression, abundance, and recruitment of telomerase are regarded as the critical factors counter-acting telomere attrition and thus determining cellular self-renewal capacity in health and disease[10].

In the human population, telomere length normally declines throughout life and has well-defined upper and lower boundaries[11–13], deviation from which at either extreme is linked to lethal diseases. Shorter telomere length is associated with reduced lifespan by mendelian randomization[14], and germline mutations in the telomerase components and related genes which result in short telomeres lead to a spectrum of fatal degenerative diseases termed telomere biology disorders (TBDs)[15] characterized by premature stem cell exhaustion. Conversely, long telomeres are associated with increased risks of various malignancies in the general population by mendelian randomization[14,16], and rare germline mutations that lead to long telomeres predispose patients to melanoma, chronic lymphoblastic leukemia and other cancers[17–20]. Despite these associations, the cellular mechanisms constraining human telomere length remain incompletely defined.

[1]Division of Hematology/Oncology and Stem Cell Program, Boston Children's Hospital, Boston, MA, USA. [2]Pediatric Oncology, Dana-Farber Cancer Institute, Boston, MA, USA. [3]Harvard Stem Cell Institute, Harvard Initiative for RNA Medicine, and Department of Pediatrics, Harvard Medical School, Boston, MA, USA. [4]Biological and Biomedical Sciences PhD Program, Harvard Medical School, Boston, MA, USA. [5]Harvard/MIT MD-PhD Program, Harvard Medical School, Boston, MA, USA. e-mail: suneet.agarwal@childrens.harvard.edu

Nuclear dNTP pools serve as common substrates for genome replication by DNA polymerases and reverse transcription by telomerase, and as such have generally been assumed to be sufficient for telomere lengthening capacity in cells. However, an emerging body of genetic and functional data suggests that dNTP metabolism impacts human telomere biology. Genetic variation in dNTP metabolism genes has been linked with telomere length by GWAS[14,21,22], and germline mutations at the thymidylate synthase (*TYMS*) locus have been found to cause dyskeratosis congenita, the prototypical TBD[23]. Despite these and other[24,25] clear genetic associations, the mechanisms and extent to which nucleotide metabolism controls telomerase activity in human cells are not well understood, in large part due to barriers in eliciting measurable changes in telomere length after acute perturbations in the native cellular context.

Here, we developed a rapid and robust human cell-based assay to dissect the metabolic regulation of telomerase reverse transcription. We reveal that nucleotide salvage efficiency bidirectionally controls telomerase activity and telomere length in human cells, to a degree as strong as that observed from manipulating core telomerase components. Overcoming limits on nucleotide salvage by deoxynucleoside kinase over-expression rapidly increased telomere length in human cell lines, and was effective in primary cells as well as cells derived from patients with TBDs. Our findings revise the current model of human telomere length regulation by demonstrating significant constraints on telomerase reverse transcriptase activity due to nucleotide salvage efficiency and dNTP levels, in a manner that may be modifiable for therapeutic benefit.

TRACE – a rapid human cell-based telomerase assay

The absence of rapid, high-throughput assays to study telomerase reverse transcription in its native cellular setting has been a major barrier to assessing the impact of metabolic perturbations and identifying therapeutically useful targets. Current telomerase assays either rely on measuring telomere length changes in cells after continuous culture requiring several weeks, or measuring enzymatic telomeric repeat addition in cell lysates using exogenous dNTPs and primers, potentially obscuring critical aspects of telomerase regulation. To overcome these barriers, we established a method to acutely interrogate the effects of cellular perturbations on telomerase activity within the nucleus at the native chromosome end, called Telomerase Rapid Assessment in the Cellular Environment, or TRACE (Fig. 1a). In TRACE, telomerase-null 293 T cells with short telomeres[25] are transfected with vectors encoding the core telomerase components, TERC and TERT (Supplementary Fig. 1a, b)[26], leading to telomerase overexpression. In this setting of supra-physiologic telomerase activity, telomerase-mediated telomere lengthening is detectable by terminal restriction fragment (TRF) Southern blot in less than 48 h (Fig. 1b, Supplementary Fig. 1c, d), yielding a quantifiable signal that can be used to measure the effects of small molecule or genetic manipulations of telomerase. To evaluate how TRACE responds to small molecules, we applied the telomerase inhibitor BIBR1532[27] for 30 h in the assay and found dose dependent decreases in telomere synthesis (Supplementary Fig. 1e, f). To study the capability of TRACE to read out genetic defects in telomerase components, we performed the assay using expression vectors encoding TBD-associated mutations in TERT[28,29] or TERC[30] and found that these pathogenic variants impaired telomere synthesis (Supplementary Fig. 1g–j). Collectively, these data demonstrate that the TRACE assay can rapidly read out small molecule and genetic modulation of telomerase activity in human cells.

Purine nucleosides inhibit telomerase

We utilized the TRACE assay to evaluate how the manipulation of nucleotide metabolism impacts telomerase reverse transcriptase activity. We supplemented cells with individual deoxynucleosides (dNs) and ribonucleosides (rNs) at a range of concentrations and found that pyrimidines drove telomerase activation in a dose dependent manner (Fig. 1c, Supplementary Fig. 1k–m), most robustly thymidine (dT) consistent with prior results[25]. In contrast, purine nucleoside supplementation caused telomerase inhibition, with the guanine nucleosides guanosine and deoxyguanosine (dG) inhibiting telomerase activity more potently than adenosine and deoxyadenosine (dA) (Fig. 1d–j). The inhibitory effect from dG supplementation was unanticipated given prior studies demonstrating that increased levels of dGTP lead to strong activation of purified telomerase enzymatic activity[9,31–33]. Interestingly, dG inhibited telomerase activity to a greater degree at 100 µM than at 500 µM (Fig. 1j), showing a dose dependent, non-linear relationship between telomerase activity and dG supplementation. Collectively, these results demonstrate that purine nucleoside supplementation can acutely inhibit telomerase reverse transcription in human cells.

PNP is required for telomerase inhibition by guanosine and deoxyguanosine

We next used the TRACE assay to ask whether metabolites of guanosine and dG mediate the observed telomerase inhibition. First, because dG might undergo 5′-phosphorylation by deoxycytidine kinase (DCK), we tested if supplementation of 2′,5′-dideoxyguanosine (2,5ddG), a dG analog which cannot be directly phosphorylated by DCK (Fig. 2a), could also inhibit telomerase activity. Similar to the effects of guanosine and dG, we saw a dose dependent inhibitory effect of 2,5ddG supplementation in the TRACE assay (Fig. 2b). These results suggest that phosphorylation of dG by DCK to form dG nucleotides is not responsible for dG's inhibitory effects on telomerase.

To evaluate the effects of nucleoside supplementation on telomere length in cells without telomerase overexpression, we treated 293 T cells and K562 cells with either 2,5ddG or guanosine. In both cases we observed dose dependent telomere shortening after 21 days in culture (Fig. 2c, d, Supplementary Fig. 2a). These results validate the TRACE assay's ability to identify non-natural compounds that cause telomere shortening when applied to cells with endogenous levels of telomerase expression.

Both guanosine and dG nucleosides are catabolized by purine nucleoside phosphorylase (PNP) to yield guanine and the associated sugar. We thus asked whether treatment with PNP inhibitors would rescue telomerase inhibition from guanine nucleoside supplementation in the TRACE assay. When we applied the PNP inhibitor ulodesine[34], we found that telomerase reverse transcriptase activity was no longer inhibited by guanosine or dG (Fig. 2e). Ulodesine alone had no effect (Fig. 2e). These results pointed to guanine, the common downstream catabolite of guanosine and dG. Surprisingly and consistent with this, we found that supplementation with guanine itself strongly inhibited telomerase activity in the TRACE assay, in a manner that could not be reversed by ulodesine (Fig. 2e). Similar results were obtained using the structurally distinct PNP inhibitor forodesine[35] (Supplementary Fig. 2b). These data reveal an inhibitory effect of guanine, whether by direct supplementation or catabolism of dG or guanosine nucleosides by PNP, on telomerase activity in human cells.

Guanine ribonucleotides inhibit telomere lengthening in human cells

We next asked whether metabolites of guanine caused the strong telomerase inhibition we observed in the TRACE assay. Guanine can either be salvaged as guanosine monophosphate (GMP) by hypoxanthine-guanine phosphoribosyltransferase (HGPRT), or further catabolized into xanthine and uric acid by guanine deaminase (GDA) and xanthine oxidase, respectively (Fig. 2f). To test whether guanine breakdown products caused telomerase inhibition, we compared the effects of directly supplementing cells with guanine, xanthine, or uric acid in the TRACE assay. Whereas guanine supplementation potently

https://doi.org/10.1038/s41467-025-58221-7

inhibited telomerase reverse transcriptase activity, xanthine and uric acid had minimal effects at doses up to 500 μM (Fig. 2g, Supplementary Fig. 2c–e). As a complementary approach to evaluate whether the accumulation of guanine catabolic products drives telomerase inhibition, we tested the xanthine oxidase inhibitor febuxostat[36] in the TRACE assay, and found it was unable to rescue telomerase activity from treatment with either dG, guanosine, or guanine (Fig. 2h). Together, these findings indicated that guanine rather than its downstream degradation products is responsible for telomerase inhibition in cells.

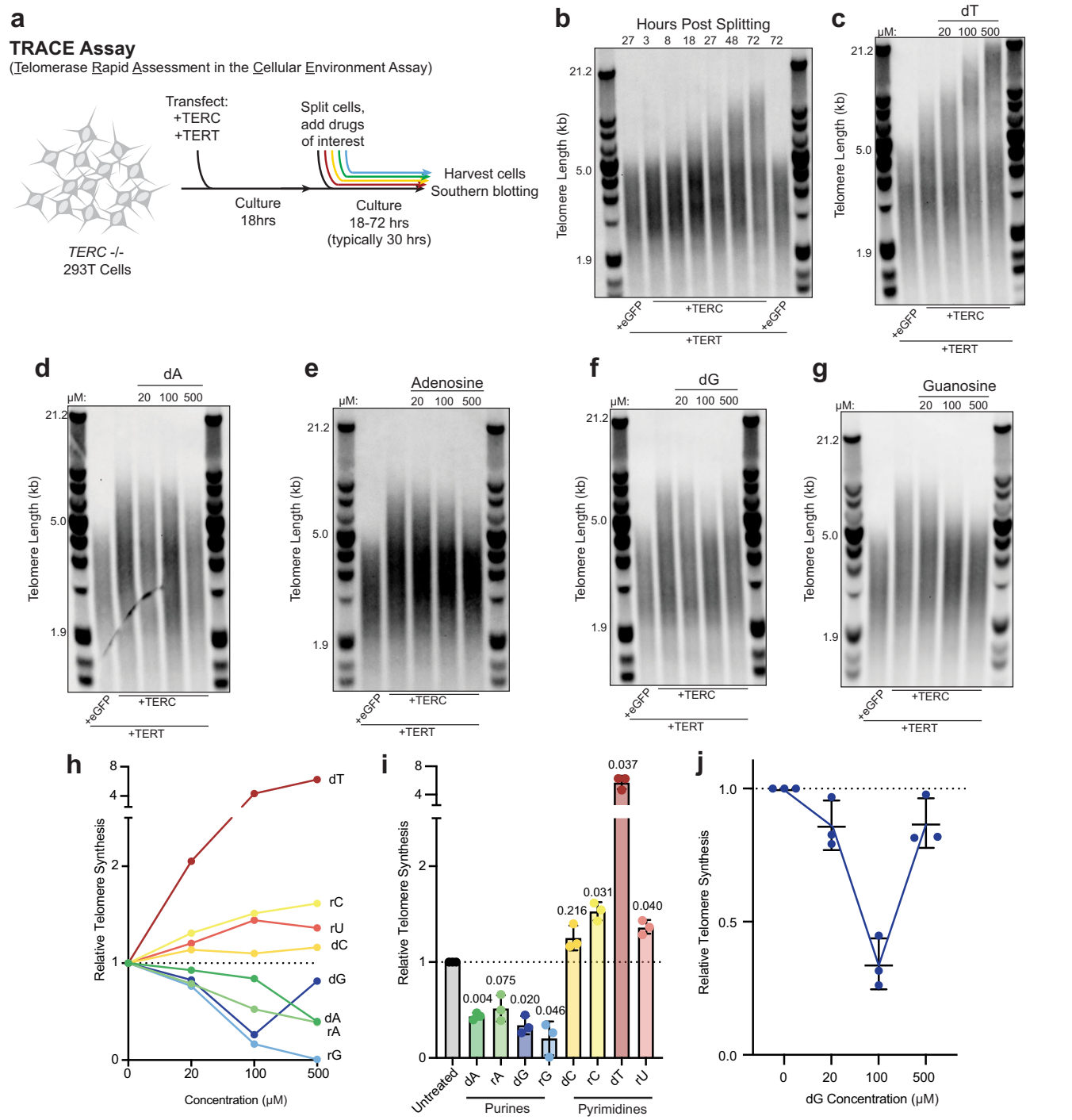

Fig. 1 | Metabolite screening by TRACE assay reveals purine nucleoside supplementation inhibits telomerase reverse transcriptase activity in human cells. **a** Diagram of TRACE assay. **b** Terminal restriction fragment Southern blot (TRF) from TRACE assay performed as follows: *TERC*−/− 293 T cells were transfected with the indicated expression vectors, cultured for 18 h, then split and harvested at the indicated timepoints after splitting. The results represent a single experiment. **c**–**g** TRFs from TRACE assay where cells were transfected as in **b**. 18 h after transfection, cells were split and supplemented as indicated for 30 h prior to harvesting. **h** Quantification of TRACE assays from **c**–**g**, and Supplementary Fig. 1i-k, displayed as the relative telomere synthesis compared to untreated cells. **i** Quantification of TRACE assay. Cells were treated with the indicated compounds at the following doses: dG, 100 μM; all other compounds, 500 μM. Experiment performed in biological triplicate. *P* values compared with untreated cells were calculated using RM one-way ANOVA with Geisser-Greenhouse correction and Dunnett's multiple comparison test. Includes data from **c**–**h** and Supplementary Fig. 1i–k. **j** Quantification of data from **f**, performed in biological triplicate. In **i**-**j**, data are presented as means; error bars indicate s.d. rC, cytidine; rU, uridine; dC, deoxycytidine; dA, deoxyadenosine; rA, adenosine; rG, guanosine. Source data are provided as a Source Data file.

https://doi.org/10.1038/s41467-025-58221-7

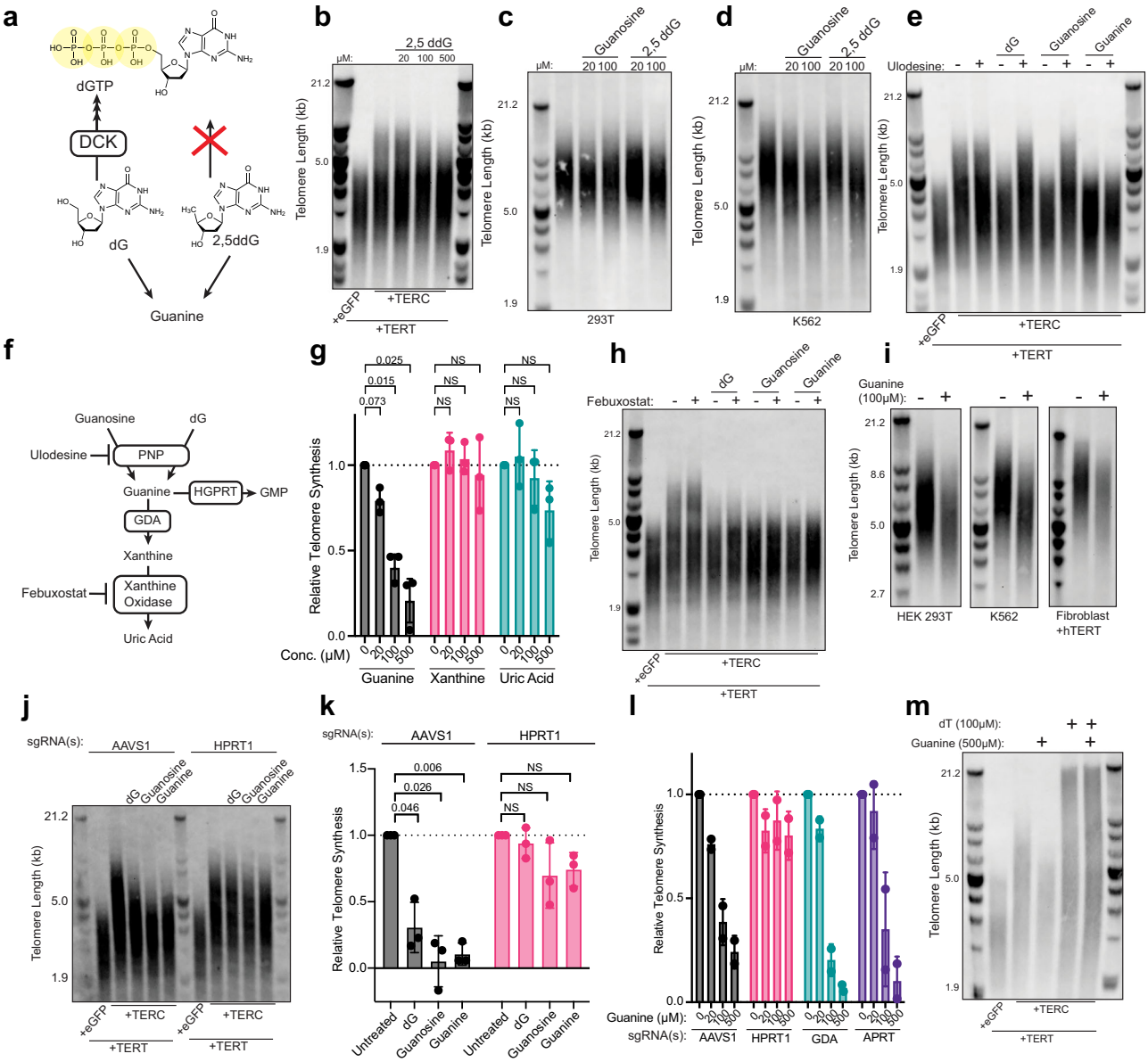

Fig. 2 | Metabolism of guanosine nucleosides by PNP and HGPRT to form guanine ribonucleotides inhibits telomerase reverse transcriptase activity and shortens telomeres. a Schematic of metabolic pathways for dG and 2,5ddG. **b** TRF from TRACE assay performed as follows: *TERC*−/− 293 T cells were transfected with the indicated expression vectors, cultured for 18 h, then split and cultured in the indicated doses of 2,5ddG for 30 h. **c, d** TRF Southern blot of 293 T cells or K562 cells cultured in the presence of the indicated compounds and doses for 21 days. **e** TRF from TRACE assay performed as in **b**. Doses of compounds: ulodesine, 1 μM; dG, 100 μM; guanosine, 500 μM; guanine, 500 μM. **f** Schematic of guanine nucleoside salvage and catabolism. **g** Quantification of TRF from TRACE assay performed as in **b** with the indicated doses of guanine, uric acid, and xanthine. See Supplementary Fig. 2b–d for corresponding representative TRFs. Experiment performed in biological triplicate. *P*-values calculated for each compound using an RM one-way ANOVA with the Geisser-Greenhouse correction and Dunnett's multiple comparisons test. **h** TRF from TRACE assay performed as in **b**. Doses of compounds: febuxostat, 100 μM; dG, 100 μM; guanosine, 500 μM; guanine, 500 μM. **i** TRF of indicated cells cultured with or without 100 μM supplemented guanine for three weeks. Representative TRF shown from three biological replicates. **j** TRF from TRACE assay performed on *TERC*−/− 293 T targeted with the indicated sgRNA(s). Assay performed as in **b**. dG, 100 μM; guanosine, 500 μM; guanine, 500 μM. Representative TRF shown from three biological replicates. **k** Quantification of **j**. dG, 100 μM; guanosine, 500 μM; guanine, 500 μM. *P*-values calculated for each genotype using an RM one-way ANOVA with the Geisser-Greenhouse correction and Dunnett's multiple comparisons test., **l** Quantification of TRF from TRACE assay performed using *TERC*−/− 293 T targeted with the indicated sgRNA(s). Assay performed as in **b**. See Supplementary Fig. 2h, i for corresponding representative TRFs. Experiment performed in biological duplicate. *P*-values calculated with a one-way ANOVA with Dunnett's multiple comparisons test. **m** TRF from TRACE assay performed as in **b**. Representative TRF shown from three biological replicates. Data in **g, k**, and **l** are presented as means and error bars indicate s.d. The results from c-e represent single experiments. Source data are provided as a Source Data file.

To study these effects under conditions with physiologic telomerase expression, we treated unmanipulated 293 T or K562 cells with 100 μM guanine for 21 days and found reproducible telomere shortening (Fig. 2i, Supplementary Fig. 2f). To test this in diploid primary cells, we treated normal human fibroblasts in which TERT was stably expressed with guanine for 21 days, and similarly observed inhibition of telomere lengthening (Fig. 2i, Supplementary Fig. 2f). Collectively, these results demonstrate that conversion of guanosine and dG into guanine causes inhibition of telomerase reverse transcription, and show that guanine supplementation itself can shorten telomeres in human cancer cell lines with endogenous telomerase levels.

We next asked if guanine supplementation requires its salvage into cellular ribonucleotide pools via HGPRT to cause telomerase inhibition. Using CRISPR/Cas9, we generated *HPRT1* deficient *TERC*−/− 293 T cells and verified efficient on-target gene inactivation (Supplementary Fig. 2g, h). We similarly used CRISPR/Cas9 to generate *TERC*−/− 293 T cells deficient for *APRT*, encoding adenine phosphoribosyltransferase which converts adenine to AMP, and *GDA* encoding guanine deaminase which catabolizes guanine to xanthine (Supplementary Fig. 2i). The *AAVS1* safe harbor locus was targeted as a control. Using the TRACE assay we found that, relative to control cells, the inhibitory effects of guanosine, dG and guanine on telomerase activity were abrogated after *HPRT1* inactivation (Fig. 2j, k). In comparison, telomerase inhibition by guanine in *GDA*- or *APRT*-targeted cells was similar to controls (Fig. 2l, Supplementary Fig. 2j, k). Collectively, these data support a model where treatment with guanosine, dG, or guanine leads to inhibition of telomerase reverse transcriptase activity via the salvage of guanine by HGPRT to form guanine ribonucleotides.

Guanine salvage into ribonucleotide pools has been shown to reduce dNTP levels including dTTP in human cells[37]. dTTP levels are important for telomere length control[25], and can be increased by supplementing cells with dT. Therefore, we asked if the inhibitory effects of guanine treatment on telomerase could be overcome by dT supplementation. Using the TRACE assay, we found that dT supplementation fully rescued guanine-mediated telomerase inhibition (Fig. 2m). Taken together, our results support a model wherein guanine supplementation results in GMP accumulation via HGPRT salvage, which in turn depletes dNTPs needed for telomerase reverse transcription, thus shortening telomere length. Furthermore, combined with our observations of guanine-mediated telomere attrition in the setting of endogenous telomerase expression (Fig. 2i, Supplementary Fig. 2f), these data indicate that telomerase activity is constrained in human cells by dNTP substrate availability.

DCK inefficiently salvages dG to promote telomerase activation

Our data unexpectedly demonstrates that dG nucleoside supplementation inhibits telomerase via formation of guanosine ribonucleotides. However, in our original TRACE metabolite screen (Fig. 1h), we observed that at high doses dG supplementation had a diminished inhibitory effect on telomerase, with 100 μM dG inhibiting telomerase activity to a greater degree compared to 500 μM dG. We repeated this analysis using a broader dG dose range, and again found that while 100 μM dG strongly inhibited telomerase activity, 500 μM had a smaller inhibitory effect (Fig. 3a). Remarkably, 2.5 mM dG increased telomere synthesis above baseline (Fig. 3a), an observation that would not be possible without TRACE due to the cytotoxicity of dG at this dose after a few days in culture. Given that dGTP is a telomerase substrate, we wondered if salvage of excess supplemented dG by DCK into dG nucleotides could underlie the increased telomerase activity observed with high dose dG, potentially counteracting the inhibitory effects on telomerase from the "default" pathway of dG breakdown into guanine (Fig. 3b). To address this question, we used a series of small molecule and genetic approaches to alter DCK function. We first inactivated *DCK* in *TERC*−/− 293 T cells using CRISPR/Cas9 (Supplementary Fig. 3a, b) and asked if inactivation of DCK could block a potential telomerase activating effect of high dose dG. Using the TRACE assay, we found that dG at high doses no longer stimulated telomerase reverse transcriptase activity in the absence of DCK (Fig. 3c). Next, we applied the DCK inhibitor DI-87[38] to cells treated with increasing doses of dG in the TRACE assay. In comparison to the effects of dG alone, we found reduced telomerase reverse transcriptase activity at 500 μM and 2.5 mM dG in the presence of DI-87 (Fig. 3c). Finally we asked if dC supplementation could prevent telomerase activation from high dose dG, because DCK is known to prefer dC as a substrate compared with dG[39], and dC supplementation has been shown to inhibit dG salvage by DCK[40] (Fig. 3b). Using the TRACE assay, we found that while dC itself had a minimal effect on telomerase activity, the addition of dC to 500 μM dG led to shorter telomeres than 500 μM dG alone (Fig. 3d). These findings rigorously demonstrate that dG at high levels can be salvaged by DCK to form deoxyguanosine nucleotides that result in net telomerase activation, on a backdrop where dG is otherwise metabolized via guanine into guanosine ribonucleotides that cause telomerase inhibition.

Given that DCK is inefficient at phosphorylating dG, we next asked if increasing cellular DCK activity would enable dG-dependent telomerase activation at lower doses. We generated DCK overexpressing *TERC*−/− 293 T cells (Supplementary Fig. 3c) for use in the TRACE assay and found that remarkably dG could now promote telomerase activation at doses as low as 20 μM, with strong activation at 80 μM. In contrast, telomerase activity in eGFP-expressing control cells remained inhibited by dG at 40 and 80 μM doses (Fig. 3e). To test whether these telomere length increases could be explained by altered cell cycle progression, we performed cell cycle analysis but found no significant differences in cells treated with 20 μM dG irrespective of DCK overexpression (Supplementary Fig. 3d–j). Furthermore, given concerns that high doses of dG might cause a DNA damage response[37], we assessed phosphorylation of CHK1 at residue serine 345 (pCHK1 S345) but found its levels to be undetectable after exposure to 20 μM dG in the presence or absence of DCK overexpression (Supplementary Fig. 3k). Collectively, these results reveal that dG nucleotide salvage capacity is limiting for telomere elongation in a manner amenable to manipulation, and that dG metabolic pathway choice dictates its net effect on telomerase activity in human cells.

SAMHD1 restricts telomerase activation from salvaged dG nucleotides

Salvage of dG into nucleotides by DCK could be promoting telomerase activity at the mono-, di-, or triphosphate levels. The dNTPase SAMHD1 restricts cellular deoxyribonucleotide *tri*phosphate levels including dGTP and is a negative regulator of telomere length[24,25] (Fig. 3b). To determine if dG salvage acts at the nucleotide triphosphate level, we asked what impact SAMHD1 disruption would have on telomerase activation after dG supplementation in the TRACE assay. In contrast to the strong telomerase inhibition from 100 μM dG seen in control cells, we found that SAMHD1 deficient *TERC*−/− 293 T cells (Supplementary Fig. 3l)[25] showed robust telomerase activation at the same dose, an effect that increased further using 500 μM dG (Fig. 3f). In contrast, when we applied guanosine or guanine to SAMHD1 deficient cells, we found that telomerase activity was inhibited to a similar degree compared to cells in which SAMHD1 was intact (Supplementary Fig. 3m). These results suggest that the telomerase activation seen after dG salvage by DCK is not only mediated by dGTP, but potently restricted by SAMHD1. To verify that the dG dependent telomerase activation in the absence of SAMHD1 was occurring via DCK salvage, we tested the effect of inhibiting DCK and found that DI-87 strongly inhibited telomerase activation in SAMHD1 deficient cells after dG treatment (Fig. 3g). Similarly, we found that dC, which competes with dG as a DCK substrate, also restricted the telomerase activation from dG in SAMHD1 deficient cells (Fig. 3g). These results indicate that the dNTPase SAMHD1 restricts telomerase activation from dG nucleotide salvage downstream of DCK and provide further support for a model where net dGTP accumulation promotes telomerase activity.

Nucleoside salvage efficiency limits telomerase activity and telomere length

Given the strong activation of telomerase from dG when we overexpressed DCK, which is inefficient at phosphorylating dG, we wondered if reprogramming cellular metabolism to drive more efficient deoxynucleoside salvage could further promote telomerase activity. The *Drosophila melanogaster* deoxynucleoside kinase (Dm-dNK) has

https://doi.org/10.1038/s41467-025-58221-7

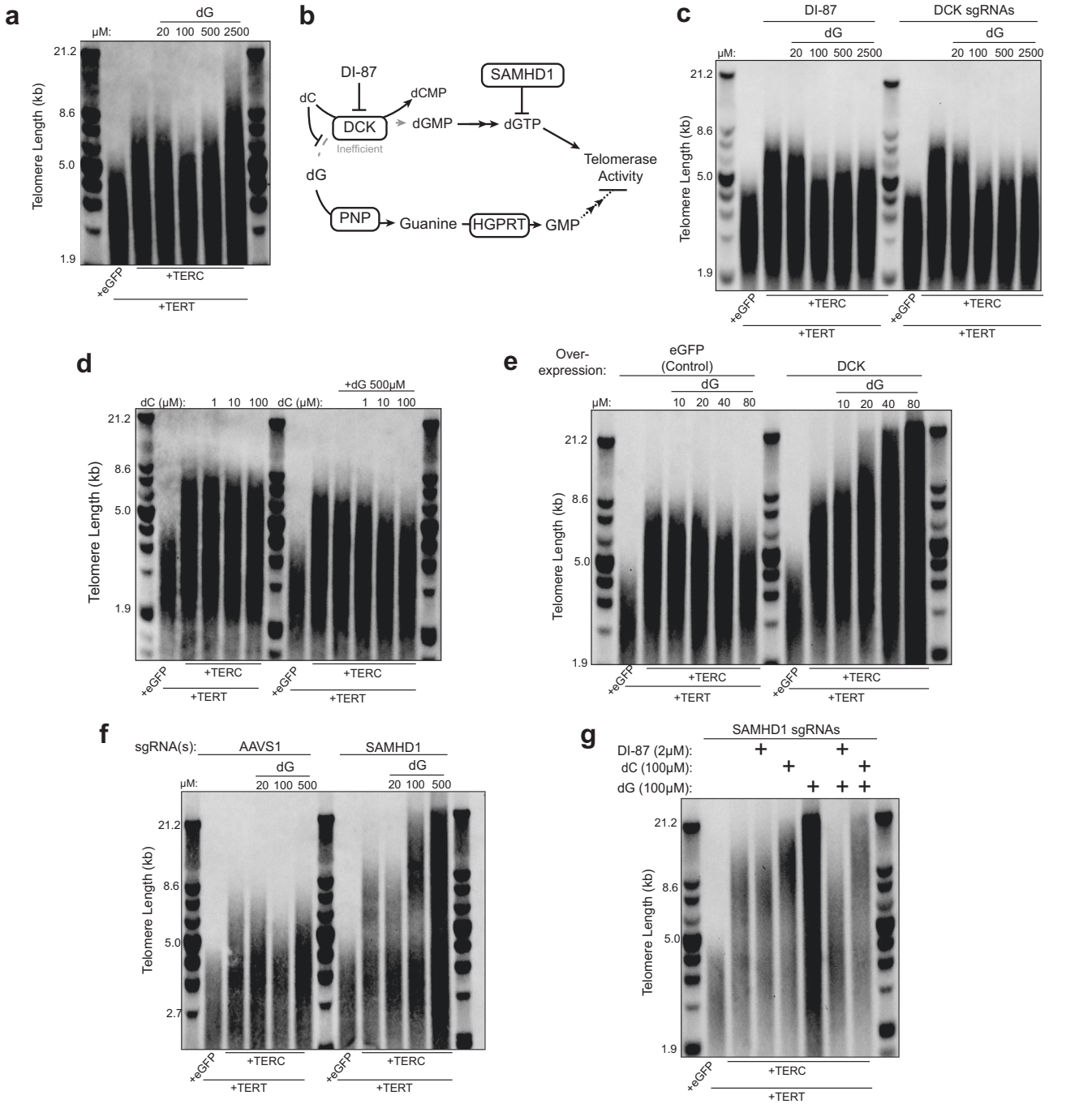

Fig. 3 | Salvage of dG nucleotides via DCK activates telomerase reverse transcription in a manner modulated by the dNTPase SAMHD1. a TRF Southern blot of TRACE assay from *TERC*−/− 293 T cells transfected with the indicated expression vectors, cultured for 18 h, then split and cultured in the indicated doses of dG for 30 h. A representative blot is shown from three biological replicates. **b** Schematic of dG salvage pathways. **c** TRF Southern blot of TRACE assay performed as in a using either *TERC*−/− 293 T cells (left), or *TERC*−/− 293 T cells which had been targeted with sgRNAs targeting *DCK* (right). Cells were treated with DI-87 at 2 μM and with dG as indicated. **d** TRF Southern blot of TRACE assay performed as in a where cells were treated with dG and dC as indicated. **e** TRF Southern blot of TRACE assay performed as in a using TERC−/− 293 T cells overexpressing eGFP or DCK. Cells were treated with dG as indicated. **f** TRF Southern blot of TRACE assay performed as in a using TERC−/− 293 T cells targeted with sgRNA(s) against *AAVS1* or *SAMHD1*. Cells were treated with dG as indicated. **g** TRF Southern blot of TRACE assay performed as in **a** using *TERC*−/− 293 T cells targeted with sgRNAs against *SAMHD1*. Cells were treated with DI-87, dC, and dG as indicated. For **c**–**g** a representative blot is shown from two biological replicates.

broad substrate specificity and eight-fold more activity on dG than DCK[41,42] (Fig. 4a). Thus we generated Dm-dNK expressing *TERC*−/− 293 T cells (Fig. 4b) and applied the TRACE assay in the setting of dG supplementation. Surprisingly, we found Dm-dNK expressing cells showed higher baseline telomerase activity compared to control eGFP expressing cells without added dG. These results indicate that overexpressing Dm-dNK to reprogram cellular nucleoside salvage capacity is sufficient to promote telomerase activation even in the absence of exogenous nucleoside supplementation (Fig. 4c, d). When we applied dG to Dm-dNK expressing cells we found a further dose dependent enhancement of telomerase activity up to 500 μM dG (Fig. 4d). In contrast to the striking telomerase activation from dG

https://doi.org/10.1038/s41467-025-58221-7

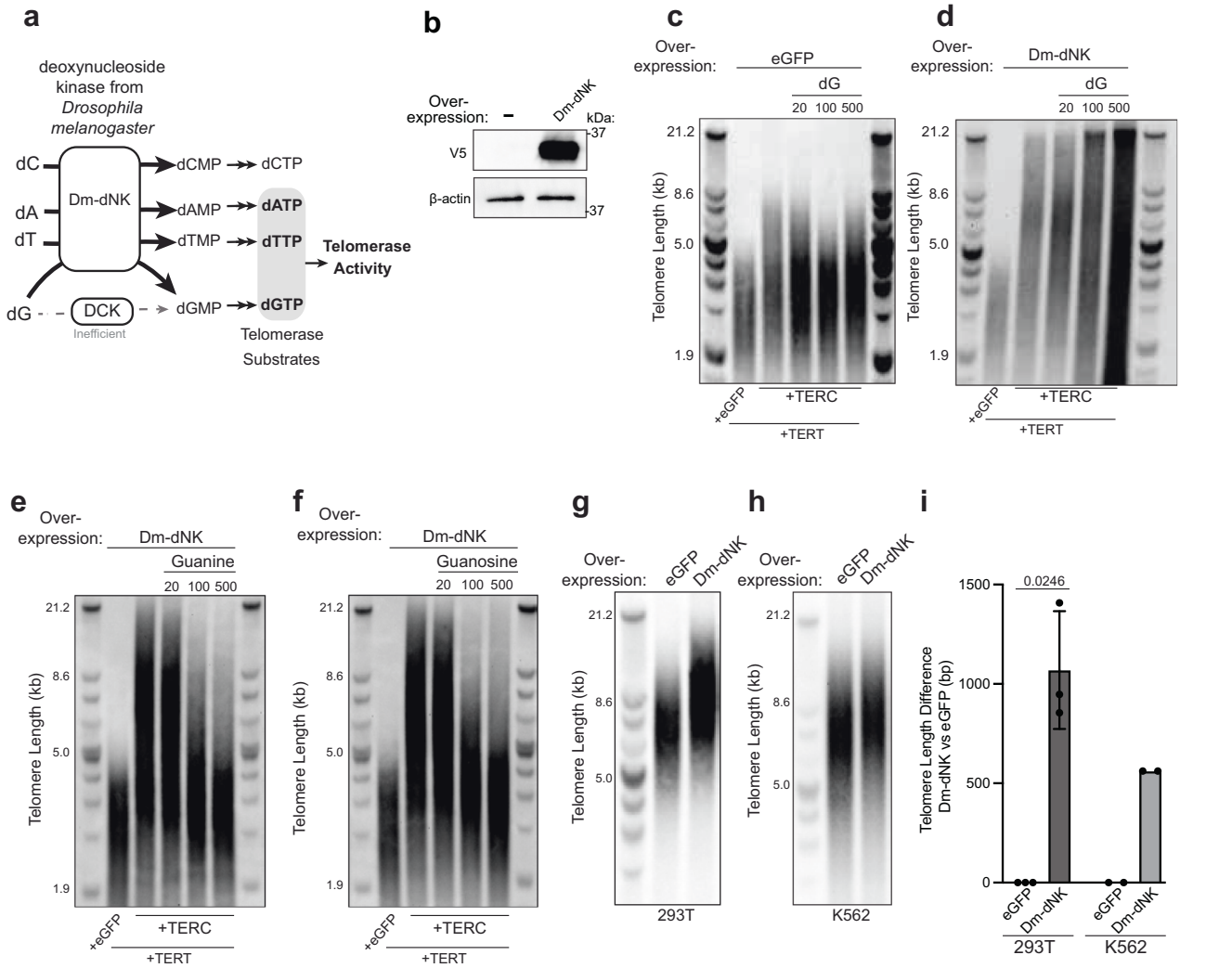

Fig. 4 | Expression of an efficient deoxynucleoside kinase from *Drosophila melanogaster* promotes telomerase activity from dG treatment and lengthens telomeres. a Schematic of Dm-dNK activity. **b** Immunoblot for V5-tagged Dm-dNK in *TERC* −/− 293 T cells stably expressing Dm-dNK. The results represent a single experiment. **c**–**f** TRF Southern blot of TRACE assay from *TERC* −/− 293 T cells overexpressing either eGFP or Dm-dNK which were transfected with the indicated doses of dG, guanine, or guanosine for 30 h. Experiments performed in biological duplicate (**c**–**e**) or biological triplicate (**f**). **g** TRF Southern blot of 293 T cells which were transduced with lentivirus for constitutive overexpression of eGFP or Dm-dNK and cultured for one month. A representative blot is shown from three biological replicates. **h** TRF Southern blot of K562 cells which were transduced with lentivirus for doxycycline inducible overexpression of eGFP or Dm-dNK and cultured for one month in the presence of 1 µg/mL of doxycycline. A representative blot is shown from two biological replicates. **i** Quantification of **g** and **h**. Data are presented as means and error bars indicate s.d. *P*-values were calculated using a paired two-sided *t* test. Source data are provided as a Source Data file.

supplementation, treatment with guanosine or guanine continued to show inhibitory effects telomere synthesis, consistent with the specificity of Dm-dNK for dNs (Fig. 4e, f). These results confirm that dG salvage into deoxyribonucleotides is limiting and stimulates telomerase activity in human cells.

We next asked whether overexpressing Dm-dNK could promote telomere lengthening in long term culture of human cells without telomerase overexpression. When we infected cells with Dm-dNK constructs and compared them with eGFP expressing control cells, we found Dm-dNK overexpression led to robust telomere lengthening in 293 T cells over 25 days of culture (Fig. 4g, i). Whereas a similar level of Dm-dNK expression (driven by a CMV promoter) was not well tolerated in K562 cells, use of a doxycycline-inducible Dm-dNK expression construct also showed telomere lengthening compared to controls (Fig. 4h, i). Taken together, these findings indicate that deoxynucleoside salvage capacity actively constrains telomere synthesis in human cells, and can be metabolically reprogrammed to increase telomerase activity and telomere length.

Manipulating deoxynucleoside salvage drives telomere lengthening in cells from TBD patients

Telomere biology disorders (TBDs) are caused by hypomorphic mutations in the core telomerase components and other telomere maintenance genes. Based on our findings showing overexpression of Dm-dNK could promote telomere lengthening, we asked if the expression of Dm-dNK could overcome genetic defects in telomere synthesis and yield telomere lengthening in cells from TBD patients. To address this question, we utilized a panel of fibroblasts from TBD patients carrying pathogenic mutations in *TERC*, *DKC1* which encodes a member of the telomerase holoenzyme, or *TINF2* which encodes a component of the telomere shelterin complex. We first determined that ectopic expression of Dm-DNK robustly increased telomere length in normal human skin fibroblasts stably expressing TERT (Fig. 5a, Supplementary Fig. 4a). Next, we overexpressed Dm-dNK in TBD patient fibroblasts expressing TERT and found striking increases in telomere length by thousands of base pairs after three weeks in culture (Fig. 5b, c). These data indicate that deoxynucleoside salvage

https://doi.org/10.1038/s41467-025-58221-7

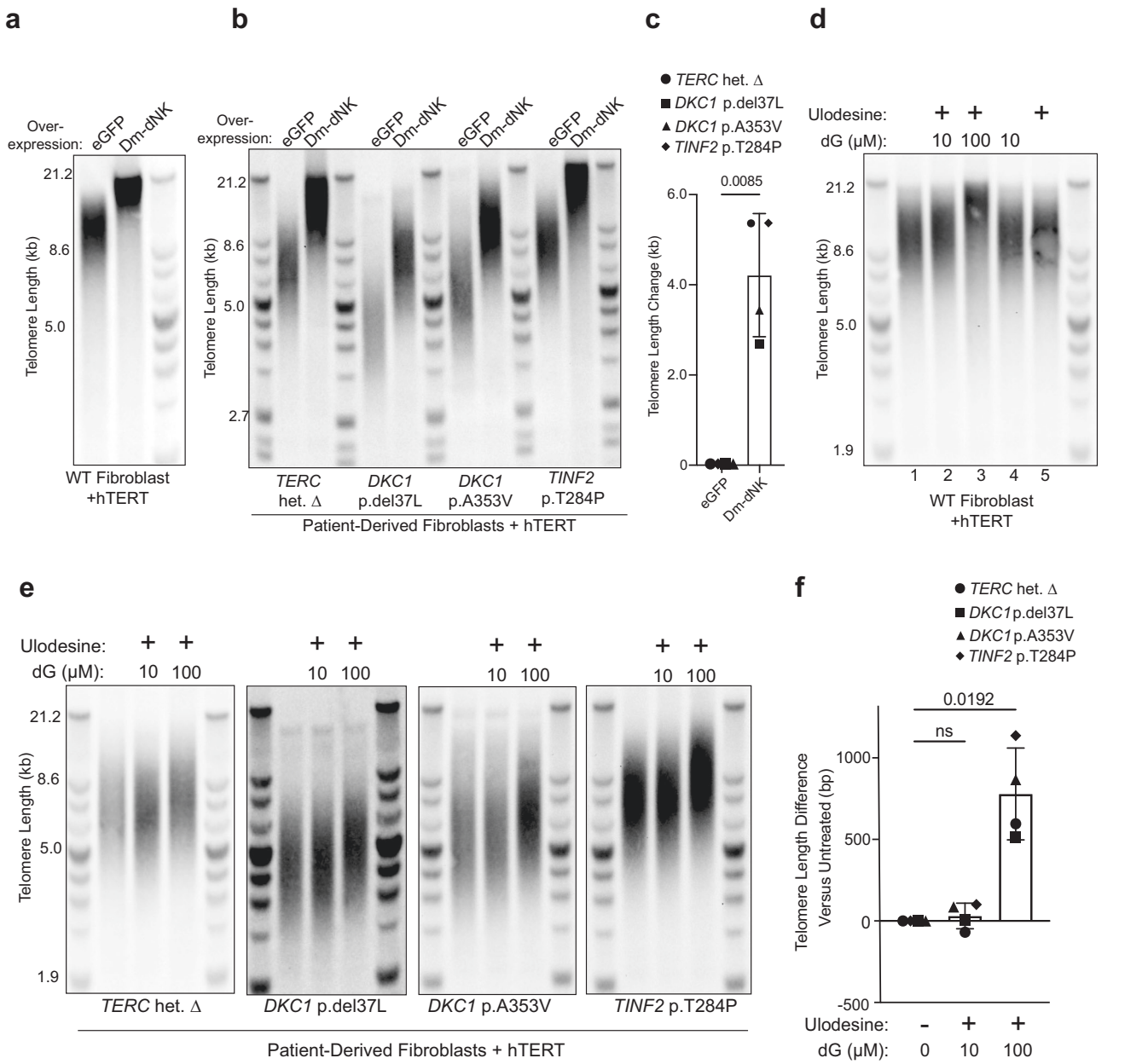

Fig. 5 | Manipulation of deoxynucleotide salvage by expressing Dm-dNK or treatment with dG plus ulodesine drives telomere lengthening in fibroblasts from patients with TBDs. a TRF Southern blot from TERT expressing fibroblasts from a healthy donor overexpressing eGFP or Dm-dNK as indicated and cultured for five weeks. **b** TRF Southern blot from TERT expressing fibroblasts from TBD patients harboring mutations in the indicated genes overexpressing eGFP or Dm-dNK as indicated and cultured for one month. **c** Quantification of median telomere length from **b**. Error bars represent s.d. *P* value was calculated using a paired two-sided *t*-test. **d** TRF Southern blot from TERT transformed fibroblasts from a healthy donor which were treated with 1 μM ulodesine and dG as indicated for three weeks. **e** TRF Southern blot from TERT transformed fibroblasts from TBD patients harboring mutations in the indicated genes which were treated with 1 μM ulodesine and dG as indicated for three weeks. **f** Quantification of median telomere length from **e**. Statistical significance determined using paired two-sided *t*-test. Error bars indicate standard deviation. The results from a and d represent single experiments. Source data are provided as a Source Data file.

capacity actively limits telomere length in human diploid cells, and that augmenting dNTP salvage overcomes disease-causing deficiencies in telomere maintenance genes and restores telomere length in cells from patients with TBDs.

Next, based on our findings showing that the pathway by which dG is metabolized influences telomerase activity, we hypothesized that shifting the balance towards deoxynucleoside salvage rather than catabolism using small molecules would drive telomere elongation in long term culture. To test this hypothesis in primary human cells, we treated normal fibroblasts stably expressing TERT with the PNP inhibitor ulodesine either alone or in combination with supplemented dG. We found that while treatment with ulodesine alone did not lead to detectable changes in telomere length, the combination of ulodesine with 100 μM dG led to robust telomere lengthening after 21 days in culture (Fig. 5d). We next asked if the combination of ulodesine and dG treatment could promote telomere lengthening in cells derived from patients with TBDs. Remarkably, we found that treatment with ulodesine and 100 μM dG for 21 days drove telomere lengthening across all mutant genotypes tested (Fig. 5e, f). Under these conditions, we found no difference in cell growth (measured as population doublings) or cell-cycle progression in two of the four patient fibroblasts, but a reduction in growth and prolongation of S-phase for the other two fibroblasts (Supplementary

https://doi.org/10.1038/s41467-025-58221-7

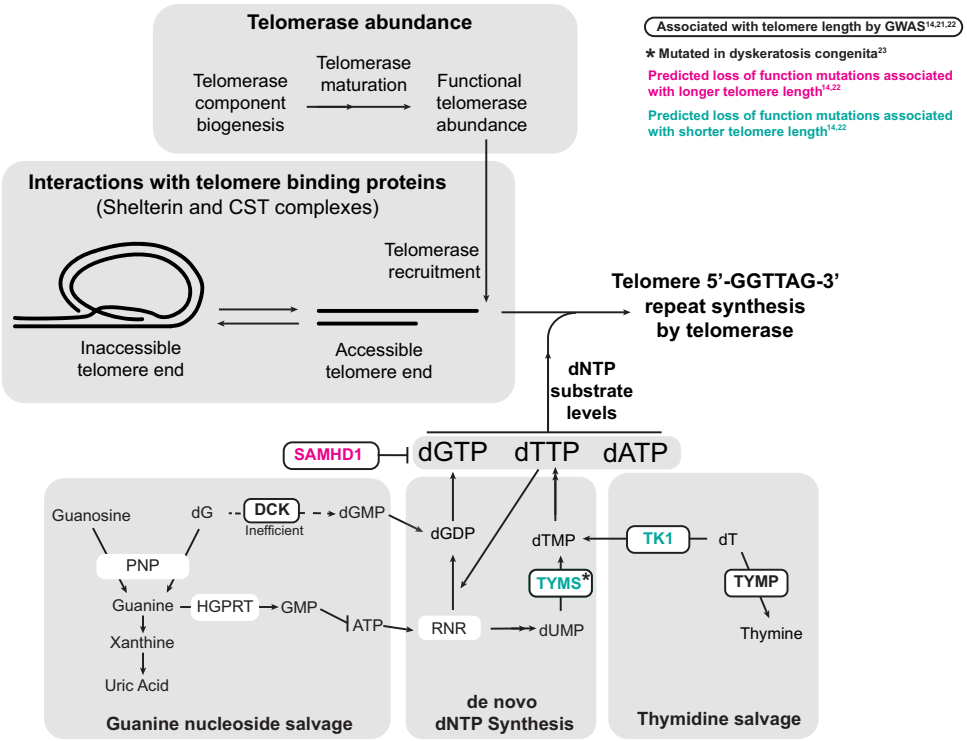

Fig. 6 | An updated model of human telomere length regulation. To date, most data indicate that human telomere length is regulated by (1) the abundance of telomerase holoenzyme and (2) its interplay with telomere binding proteins. Based on the current findings and emerging human genetic data, we propose a revised model encompassing a third critical dimension of telomere length regulation in human cells: control of dNTP substrate levels available for telomere 5′-GGTTAG-3′ repeat synthesis by telomerase. dNTP substrate accumulation is limited by salvage efficiency including (a) deoxyguanosine (dG) metabolism by DCK, and (b) thymidine (dT) conversion to dTTP via TK1[25]. dTTP can enhance dGTP production by allosteric binding to ribonucleotide reductase (RNR). Overcoming salvage constraints through dG or dT supplementation or by augmenting kinase activity robustly increases telomerase activity and telomere length. Conversely, guanine nucleoside metabolism via PNP and HGPRT to form guanosine ribonucleotides decreases telomere length, potentially by inhibiting RNR and depletion of dNTPs. Mutations that impair dTTP de novo synthesis lead to reduced telomerase substrate levels and impaired telomerase activity, as observed in patients with TYMS locus mutations who develop dyskeratosis congenita[23]. The dNTPase SAMHD1 prevents the accumulation of telomerase dNTP substrates and restricts telomerase activity. Our model provides a mechanistic framework for the recent association between genetic variation in dNTP metabolism genes and telomere length in states of health and disease.

Fig. 4b–m). None of the cultures showed increases in pCHK1 (S345) after dG plus ulodesine, indicating a lack of DNA damage response induction (Supplementary Fig. 4n, o). Together, these data indicate that the observed telomere length increases after dG and ulodesine treatment cannot be explained by changes in cell growth or S-phase progression, and do not trigger DNA damage responses. Collectively, these findings indicate that deoxynucleotide salvage limits telomere lengthening in human cells, and that genetic or small molecule-based reprogramming of deoxynucleoside salvage can promote telomere restoration in the setting of TBD-causing genetic defects.

Discussion

Telomere length must be kept within a tight window to maintain human health. Genetic dysregulation of telomere length homeostasis leading to either aberrantly short or long telomeres predisposes to lethal diseases. Telomere length is generally considered to be governed by the expression and abundance of telomerase, and the recruitment of telomerase to the chromosome end by shelterin proteins[10]. Here, we reveal that reverse transcription by telomerase in human cells is constrained by the availability of dNTP substrates for 5′-GGTTAG-3′ repeat synthesis. Based on our findings, we propose an updated model for the regulation of telomerase reverse transcription, wherein modulation of nucleotide synthesis and salvage plays an active, critical role in human telomere length homeostasis in normal and disease states (Fig. 6). While strategies to therapeutically target canonical regulators of telomerase – expression, abundance, recruitment – have met with limited success to date, our findings suggest that well-trodden paths of pharmacologically manipulating nucleotide synthesis or salvage could lead to new treatments for genetic telomere diseases and other degenerative disorders.

This work was stimulated by several emerging lines of human genetic evidence implicating nucleotide metabolism in telomere length control[14,21,23], hitherto lacking mechanistic explanations consistent with prevailing models of telomerase regulation. Independent genetic and functional studies have converged on thymidine metabolism as the central player in the regulation of human telomerase activity and telomere length[23,25]. These findings appear to contrast prior studies using purified telomerase showing that dGTP rather than dTTP plays a dominant role in the control of enzymatic activity[9,31–33]. Here, we sought to comprehensively determine the relationship between nucleotide metabolism and telomerase reverse transcriptase activity in intact human cells and developed the TRACE assay. TRACE enables detection of telomere length changes in human cells within 48 h and can be applied to study the impact of metabolic perturbations on telomerase reverse transcriptase activity. We were thus able to screen nucleoside metabolites for their effects on telomere synthesis and identified a bidirectional and limiting role of guanine nucleoside salvage in telomerase regulation. Our findings indicate that the low efficiency of dG phosphorylation by DCK restricts dG nucleotide accumulation and limits telomerase activation from dG supplementation. In the TRACE assay, very high doses of dG were able to overcome this inefficiency and promote telomerase activation. Furthermore, increasing the efficiency of dG salvage by DCK overexpression yielded potent telomerase activation. These data indicate

that dGTP accumulation drives strong telomerase activation in human cells, in line with the effects of dGTP levels on purified human telomerase[31–33] and in yeast cells[43]. These results are also consistent with recent observations of negative regulation of telomere length by the dNTPase SAMHD1, which preferentially degrades dGTP[24,25]. Along these lines, the sensitivity of telomerase to dGTP may contribute to the telomerase activation seen after dT supplementation[25]. dTTP has been shown to allosterically act on ribonucleotide reductase (RNR) to increase dGTP production[44]. The upregulation of dGTP after dT treatment may offer an explanation for the surprising finding that telomere repeat synthesis is stimulated by dT supplementation even when telomerase is modified to no longer use dTTP as a substrate[25]. Of note, the efficiency of dT salvage by TK1 is orders of magnitude higher than the efficiency of dG salvage by DCK[41,45,46], potentially explaining the more robust effect of dT than dG supplementation on telomere elongation in cells. Together, under this model, our findings provide a mechanism for human GWAS data linking the cytosolic deoxynucleoside kinases TK1 and DCK with telomere length[14,21,22], acting at the level of nucleoside salvage efficiency. Overcoming normal human physiologic limits on salvage capacity by overexpressing a highly efficient deoxynucleotide kinase from *Drosophila melanogaster* drove robust telomere lengthening, including cells derived from TBD patients. In sum, these findings reveal that deoxynucleoside salvage efficiency actively constrains telomere synthesis by telomerase under physiological conditions, and can be manipulated to overcome impaired telomere maintenance in the setting of TBD-causing genetic defects.

In addition to revealing the importance of deoxynucleoside salvage capacity for telomerase regulation, we also surprisingly found that guanine or guanine nucleoside supplementation led to telomerase inhibition, and guanine treatment drove telomere shortening across multiple cell types including cancer cell lines. Guanine supplementation has been found to deplete dNTPs including dTTP and dGTP[37,47]. While the mechanism underlying dNTP depletion from guanine supplementation has not been established, guanine salvage into ribonucleotides pools has been shown to reduce ATP levels in human cells[37,47]. ATP is an allosteric activator of RNR[44] which is the rate-limiting enzyme in the de novo dNTP synthesis pathway, including the telomerase substrates dGTP and dTTP. Based on this model, we hypothesized that guanine could be inhibiting telomerase by reducing dNTP levels, and asked if upregulating dNTP synthesis could rescue telomerase inhibition in guanine treated cells. We found that augmenting dNTP production by supplementing with dT could fully rescue cells from guanine-mediated telomerase inhibition. These results support a model whereby guanine salvage inhibits telomerase by limiting dNTP availability for telomere synthesis. More broadly, our data showing that dG nucleoside supplementation bidirectionally controls telomerase activity can be unified under a model wherein the dNTP substrates required by telomerase are either increased or decreased, depending on net dG metabolism into guanosine deoxyribonucleotides versus ribonucleotides. (Fig. 6).

Telomerase activation is a critical step in tumorigenesis in many cancers, and effective anti-neoplastic telomerase inhibitors have been long-sought after but remain largely elusive. dNTP levels are elevated in most cancers[48] by means including the upregulation of the rate limiting thymidine salvage enzyme TK1. Similarly, deoxynucleoside kinases are expressed in many viruses which cause human disease including the oncogenic viruses Epstein-Barr virus and Human Herpesvirus-8[49] which also upregulate telomerase activity as part of their progression[50]. It has been proposed that the increased dNTP levels in cancer cells enables efficient genome replication and frequent cell divisions. Based on our data, it is also possible that elevated dNTP levels provide a selective advantage to tumor cells by lifting a metabolic constraint on telomere synthesis by telomerase. Several nucleotide analog chemotherapy drugs are known to inhibit dNTP synthesis such as gemcitabine, clofarabine, and 5-fluorouracil, and we therefore speculate that telomerase inhibition may contribute to their anti-tumor activity. The intersection between nucleotide metabolism and telomerase activity offers a new avenue to examine how cellular self-renewal limits are bypassed in chronic viral infections and tumorigenesis, and how this may be interrupted therapeutically.

Manipulation of dNTP metabolism also plays an essential role in the treatment of a variety of disorders beyond cancer, such as purine synthesis inhibitors azathioprine and mycophenolate mofetil in autoimmune disorders, uridine monophosphate in patients with CAD deficiency, and deoxypyrimidines in patients with TK2 deficiency. Based on the robust telomere lengthening we observed from overexpressing DmdNK as well as from using ulodesine plus dG in primary human cells from patients with genetically-diverse TBDs, our data suggest that strategies to shift deoxynucleoside metabolism towards dNTP accumulation could be a promising therapeutic strategy to augment telomerase activity in TBDs. PNP inhibitors have been shown to be well-tolerated, and to increase serum dG levels and cellular dGTP levels[51,52], and thus based on our data, may be able to promote telomere lengthening as a single agent. However, dNTPs are broadly utilized substrates for diverse cellular functions including nuclear and mitochondrial DNA replication and repair, and their manipulation is known to impact cell growth and proliferation in a dose-dependent manner[37]. Translational efforts to manipulate deoxynucleotide metabolism and define a therapeutic window in TBDs will therefore require scrutiny of potential impacts on the activity and fidelity of the myriad cellular factors regulating these functions. Finally, attention will need to be paid to the composition of telomere repeat sequences themselves after dG or dT supplementation, exploiting emerging sequencing technologies[53–55].

Nuclear dNTP pools serve as common substrates for genome replication by DNA polymerases and for telomere synthesis by telomerase, yet these DNA synthesis machines must perform fundamentally different tasks. While replicative DNA polymerases copy billions of base pairs of sequence with high fidelity within hours during S phase of the cell cycle, telomerase activity is tightly tied to the rate of telomere attrition which is estimated to be ~50–100 base pairs per cell division at each chromosome end[5,56]. Additionally, unlike replicative DNA polymerases, telomerase has no defined endpoint for telomere repeat synthesis once it has begun. Tight regulation of TERC and TERT expression and control of telomere end accessibility by the shelterin and CST complexes have long been proposed to explain the homeostatic limit of human telomere length[57]. However, in our recent[25] and present work collectively, we have overcome this limit through manipulation of dNTP levels using four different approaches: thymidine supplementation, dG supplementation plus PNP inhibition, SAMHD1 inactivation, and deoxynucleoside kinase overexpression. Nuclear dNTP pool homeostasis is under competing selective pressures including the need to maintain genome fidelity and to restrict the proliferation of DNA viruses, retroviruses, and selfish genetic elements. Given the sensitivity of cellular telomerase activity to changes in dNTP metabolism that we observed in this study, we propose that selective pressures on cellular dNTP levels may have shaped telomere length homeostasis throughout evolution. Conversely, the need to maintain reverse transcription by telomerase may contribute to the lower bound of tolerable dNTP levels: further reductions of dNTPs can cause diseases of telomerase insufficiency, as seen in patients with inherited *TYMS* locus mutations who develop dyskeratosis congenita[23]. We expect that this telomerase-inclusive perspective will offer new insights on how competing constraints on nucleotide flux have impacted cellular metabolism and genome integrity throughout evolution.

Methods

Materials and correspondence

Correspondence and material requests should be addressed to the corresponding author.

Patient material

Biological samples were procured under Boston Children's Hospital Institutional Review Board-approved protocols, after written informed consent in accordance with the Declaration of Helsinki. The patient with mutation of the *TINF2* gene presented with dyskeratosis congenita and bone marrow failure in early childhood, consistent with the mutation leading to the p.T284P amino acid change in the 'hot spot' region of *TINF2*, a site where mutations are frequently associated with the TBD dyskeratosis congenita.

Cell culture

293 T cells (American Type Culture Collection, ATCC) were cultured in Dulbecco's Modified Eagle Medium (DMEM, Gibco) supplemented with 10% fetal bovine serum, MEM Non-Essential Amino Acids (Gibco), L-glutamate (Corning), and penicillin/streptomycin (Corning) and subcultured using trypsin (Gibco). K562 cells (American Type Culture Collection, ATCC) were cultured in RPMI 1640 supplemented with 10% fetal bovine serum, MEM Non-Essential Amino Acids (Gibco), L-glutamate (Corning), and penicillin/streptomycin (Corning). Fibroblasts cells were cultured in Dulbecco's Modified Eagle Medium (DMEM, Gibco) supplemented with 15% fetal bovine serum, MEM Non-Essential Amino Acids (Gibco), L-glutamate (Corning), and penicillin/streptomycin (Corning) and subcultured using trypsin (Gibco). The normal human fibroblast line NHSF2 was a gift from A. Klingelhutz, University of Iowa. The TBD patient fibroblasts (GM01774[58]) carrying the DKC1 del37L mutation were obtained from the Coriell Cell Repository. The TBD patient fibroblasts with the DKC1 A353V mutation have been described[59]. The TBD patient fibroblasts with the *TERC*$^{+/-}$ 821 base pair deletion have been described[60]. The TBD patient fibroblasts with the TIN2 p.T284P mutation were generated by culturing punch biopsies under glass coverslips until fibroblast outgrowths were apparent. All fibroblast lines were infected with pCW57.1 TERT lentivirus, selected in puromycin, and cultured in the presence of 1 µg/ml doxycycline (Sigma-Aldrich) during experimental perturbations. Lentiviral transduction was performed via spinfection at 931 G for 2 h in media supplemented with protamine sulfate (Sigma-Aldrich) at 10 µg/ml. 24 h after removal of virus containing media, cells were selected using blasticidin (InvivoGen) at 10µg/ml for 5-10 days or puromycin (Sigma-Aldrich) at 1µg/ml for 4–7 days. A description of the small molecules used in this study is available in Supplementary Table 1.

Lentivirus production

293 T cells were transfected with psPAX2 and pMD2.G in addition to the appropriate transfer vector using Lipofectamine 2000 (Invitrogen) per the manufacturer's instructions. Lentivirus containing media was harvested 48 and 72 h after transfection, filtered using 0.45 µM filters (VWR International), and stored at −80 °C until use.

TRACE assay

On the evening prior to transfection, *TERC*−/− 293 T cells were plated at 0.75×10^6 cells per ml of media into a six well plate. The following day, cell media was replaced approximately one hour prior to transfection. Transfection was performed as follows. For each well of a six well plate, 8 µl of Lipofectamine 2000 (Invitrogen) was mixed with 150ul of Opti-MEM serum free media (Gibco) and incubated for 5 min. In a separate tube, 416 ng pcDNA-3xHA-TERT and 2083 ng of either pBS-U3-TERC or pMAX-eGFP as indicated were mixed into 150 µl of Opti-MEM. These two solutions were then combined, mixed gently, and incubated for 5 min followed by dropwise addition to cells. 18 h after transfection, cells were split into treatment conditions and cultured for 30 h unless otherwise indicated. Cells were then harvested and pellets were stored at −80 °C until DNA isolation and terminal restriction fragment length analysis (described below).

Terminal restriction fragment length analysis

DNA was isolated from cell pellets using the Pure Link Genomic DNA Miniprep kit (Invitrogen). 0.5–3 µg of DNA was digested with RsaI (NEB) and HinfI (NEB) for 2 h at 37 °C. DNA was then separated by electrophoresis on a 0.6% agarose gel followed by Southern blotting onto Hybond-N+ membrane (Amersham). Detection was performed using the TeloTAGGG Telomere Length assay Kit (Roche) using the provided probe at the recommended concentration or a probe complementary to the C-rich strand of the telomere synthesized by annealing the CCCTAA-rich strand probe template to the universal priming oligonucleotide (see Supplementary Table 2), filling in with Exo- Klenow Fragment (NEB) and a dNTP mix containing DIG-11-dUTP (Roche), blunting with T4 DNA Polymerase (NEB), and degrading the template using Lambda Exonuclease (NEB)[61]. Where indicated, Southern blots were stripped using two washes with 0.2 M NaOH and 0.1% sodium dodecyl sulfate (SDS) at 37 °C for 15 min with shaking followed by detection as described above. Telomere length quantification was performed with the WALTER webtool (v2.0)[62]. TRACE assay experiments were quantified using ImageJ (Version 2.9.0/1.54 f) as follows: First, calculate the ratio (R) of signal above 5 kb (largely newly synthesized telomere) to below 5 kb (largely pre-existing telomere signal for TERC−/− 293 T cells) for each sample. Then, to calculate background normalized ratios (Rb), for each sample expressing TERC, subtract R for eGFP expressing cells on the same blot (removing background signal contribution) from sample R. Then, to calculate the relative telomere synthesis for a given sample, divide the Rb of experimental samples by the untreated control sample on the same blot (normalizing relative to untreated). Statistical analysis was performed using GraphPad Prism (version 10.0.0).

RT-qPCR

Total cellular RNA was harvested from 293 T and *TERC*−/− 293 T cells using Trizol (Thermo Fisher) according to the manufacturer's protocol. RNA was then DNase treated to remove genomic DNA with the Turbo DNase Kit according to the manufacturer's protocol (Thermo Fisher). cDNA synthesis was achieved using Superscript III Reverse Transcriptase with random hexamer priming (Thermo Fisher). RT-qPCR was then conducted on cDNA using SsoAdvanced Universal SYBR Green Supermix (Bio-Rad) according to the manufacturer's instructions on a Bio-Rad CFX96 real-time PCR machine. Relative gene expression was quantified using standard ΔΔCt methodology.

Cell cycle analysis by DAPI staining and flow cytometry

Approximately 1×10^6 cells per treatment condition were fixed in 70% (*v/v*) ethanol then stained for DNA content with DAPI followed by flow cytometry analysis on an LSR II analyzer (BD Biosciences) using BD FACSDiva version (8.0.2). Twenty thousand *TERC*−/− 293 T cells and 10,000 patient fibroblast cells were analyzed per sample. Cells were gated on forward versus side scatter and cell cycle phases were first gated in a control sample for each comparison and applied to all samples as described in Supplementary Fig. 3d–f using FlowJo version 10.9.0.

Immunoblotting

Cells were lysed in RIPA buffer (Thermo Fisher) supplemented with complete protease inhibitor cocktail (Roche) and lysates were quantified using the Bio-Rad DC protein quantification assay according to the manufacturer's protocol. For immunoblots assessing DNA damage markers (Supplementary Fig. 3k, Supplementary Fig. 4n, o), 15 µg protein was mixed with 2X Laemmli buffer (Bio-Rad) and run on 4–20% tris-glycine SDS gel (Bio-Rad), followed by transfer to a polyvinylidene difluoride membrane. For all other immunoblots, 20 µg protein lysate was used. HGPRT was detected using a rabbit primary antibody from Protein Tech (17758-1-AP) at a 1:1000 dilution. TERT was detected using a rabbit primary antibody from Rockland (600-401-252) at a 1:1000

dilution. DCK was detected using a rabbit primary antibody from GeneTex (GTX102800) at a 1:1000 dilution. SAMHD1 was detected using a rabbit primary antibody from Abcam (ab67820) at a 1:500 dilution. V5-tagged Dm-dNK was detected using an anti-V5 mouse primary antibody from Invitrogen (SV5-Pk1) at a 1:1000 dilution. pCHK1 (S345) was detected using a rabbit primary antibody from Cell Signaling Technology at a 1:1000 dilution. Rabbit primary antibodies were detected using horseradish peroxidase-conjugated goat anti-rabbit IgG secondary antibody from Abcam (ab6721) at a 1:5000 dilution. Mouse primary antibodies were detected using horseradish peroxidase-conjugated goat anti-mouse IgG secondary antibody from Invitrogen (31430) at a 1:5000 dilution. Blots were imaged by chemiluminescence on a ChemiDoc Imaging system (Bio-Rad).

CRISPR/Cas9 gene editing

Gene editing was performed using the Neon Electroporation Kit (Invitrogen) by complexing 37 pmol Alt-R S.p. Cas9 Nuclease V3 (IDT) and 50 pmol chemically modified sgRNA(s) (Synthego) at room temperature for 20 min followed by addition of 200,000 cells suspended in 20 µl buffer R (Thermo Fisher Scientific) with Electroporation Enhancer (IDT). The cell mixture was electroporated using a Neon Transfection System (Thermo Fisher Scientific) using the following settings: HEK 293 T, 1200 V, 30 ms, 1 pulse; K562 1150 V, 10 ms, 3 pulses. After electroporation, cells were plated into normal media. Editing efficiency was evaluated by isolating genomic DNA from cells at least 3 days after electroporation followed by PCR amplifying the target locus. PCR products were visualized by electrophoresis on a 2% agarose gel.

Expression construct cloning

Constructs to express variants in TERT associated with TBDs were generated from the pCDNA-3xHA-hTERT vector using the Q5 site directed mutagenesis kit (NEB) and were verified by Sanger sequencing.

The DCK expression construct was cloned from 293 T cell cDNA into the pLX304 backbone by Gibson assembly using the NEB HiFi DNA assembly mix. The final construct expresses DCK with a C-terminal fusion to a V5 epitope tag which is present in the pLX304 backbone and the sequence was verified by Sanger sequencing. The cDNA was synthesized by isolating RNA from cells using TRIzol Reagent (Invitrogen), then treating RNA with TURBO DNA-free Kit (Invitrogen). Complementary DNA was synthesized using SuperScript III Reverse Transcriptase (Invitrogen) with oligo-dT priming (Invitrogen).

The PLX304-eGFP construct was generated by PCR amplifying the eGFP sequence from the pXPR_011 vector using attB-flanked primers followed by Gateway cloning (Invitrogen) according to the manufacturers protocol into the pLX304 backbone. The final construct expresses eGFP with a C-terminal fusion to the V5 epitope tag which is present in the pLX304 backbone. The sequence was verified by Sanger sequencing

The CMV driven Dm-dNK expression construct pLX304 Dm-dNK V5 was cloned from the pOpen-dromedNK plasmid into the pLX304 backbone by Gibson assembly using the NEB HiFi DNA assembly mix. The final construct expresses Dm-dNK with a C-terminal fusion to a V5 epitope tag which is present in the pLX304 backbone. The sequence was verified by Sanger sequencing

The doxycycline inducible Dm-dNK expression construct was generated by isolating the insert from the pLX304 Dm-dNK V5 using SacI (NEB) and SalI (NEB), and ligating it into the pCW57.1 backbone which had been digested with NheI (NEB) and SalI (NEB) using Quick Ligase (NEB) generating pCW57.1 Dm-dNK V5. The sequence was verified by Sanger sequencing. The blasticidin resistant version of this vector used in Fig. 4 was generated by digesting pCW57.1 Dm-dNK V5 with NotI and SpeI and ligating the Dm-dNK containing fragment into the pCW57-MCS1-P2A-MCS2 (Blast) vector which had also been digested with NotI and SpeI using Quick Ligase (NEB).

The doxycycline inducible eGFP expression construct was generated by PCR amplifying the eGFP sequence from the pXPR_011 vector using attB-flanked primers followed by Gateway cloning (Invitrogen) according to the manufacturers protocol into the pCW57.1 backbone. The sequence was verified by Sanger sequencing. The blasticidin resistant version of this vector used in Fig. 4 was generated by digesting pCW57.1 eGFP with NotI (NEB) and SpeI (NEB) and ligating the Dm-dNK containing fragment into the pCW57-MCS1-P2A-MCS2 (Blast) vector which had also been digested with NotI (NEB) and SpeI (NEB) using Quick ligase (NEB).

All PCR reactions required for molecular cloning were performed using the Q5 polymerase (NEB).

Plasmid sources

pXPR_011 was a gift from J. Doench and D. Root (plasmid 59702; Addgene)
pLX304 was a gift from D. Root (plasmid 25890; Addgene)
psPAX2 was a gift from D. Trono (plasmid 12260; Addgene)
pMD2.G was a gift from D. Trono (plasmid 12259; Addgene)
pBS U3-hTR-500 was a gift from K. Collins (plasmid 28170; Addgene).
pCDNA-3xHA-hTERT was a gift from S. Artandi (plasmid 51637; Addgene).
pmaxGFP was purchased from Lonza
pHIV7/SF-U3-TER-500 was previously described in ref. 60
pHIV7/SF-U3-TER-500 G319A was previously described in ref. 30
pcw57.1 TERT Puro was a gift from C. Reilly[63]
popen-dromedNK was a gift from Drew Endy & Jennifer Molloy & FreeGenes Project (plasmid 165579; Addgene)
pCW57.1 was a gift from David Root (plasmid 41393; Addgene)
pCW57-MCS1-P2A-MCS2 (Blast) was a gift from Adam Karpf (plasmid 80921; Addgene).

Reporting summary

Further information on research design is available in the Nature Portfolio Reporting Summary linked to this article.

Data availability

All data supporting the findings of this study are available within the paper and its Supplementary Information. Source data are provided with this paper.

References

1. Fagagna, Fd'Adda et al. A DNA damage checkpoint response in telomere-initiated senescence. *Nature* **426**, 194–198 (2003).
2. Takai, H., Smogorzewska, A. & Lange, T. de. DNA Damage Foci at Dysfunctional Telomeres. *Curr. Biol.* **13**, 1549–1556 (2003).
3. Olovnikov, A. M. A theory of marginotomy: The incomplete copying of template margin in enzymic synthesis of polynucleotides and biological significance of the phenomenon. *J. Theor. Biol.* **41**, 181–190 (1973).
4. Watson, J. D. Origin of Concatemeric T7DNA. *Nat. N. Biol.* **239**, 197–201 (1972).
5. Harley, C. B., Futcher, A. B. & Greider, C. W. Telomeres shorten during ageing of human fibroblasts. *Nature* **345**, 458–460 (1990).
6. Greider, C. W. & Blackburn, E. H. A telomeric sequence in the RNA of Tetrahymena telomerase required for telomere repeat synthesis. *Nature* **337**, 331–337 (1989).
7. Greider, C. W. & Blackburn, E. H. Identification of a specific telomere terminal transferase activity in Tetrahymena extracts. *Cell* **43**, 405–413 (1985).
8. Feng, J. et al. The RNA component of human telomerase. *Science* **269**, 1236–1241 (1995).

9. Morin, G. B. The human telomere terminal transferase enzyme is a ribonucleoprotein that synthesizes TTAGGG repeats. *Cell* **59**, 521–529 (1989).
10. Hockemeyer, D. & Collins, K. Control of telomerase action at human telomeres. *Nat. Struct. Mol. Biol.* **22**, 848–852 (2015).
11. Alder, J. K. et al. Diagnostic utility of telomere length testing in a hospital-based setting. *Proc. Natl. Acad. Sci. USA* **115**, E2358–E2365 (2018).
12. Aubert, G., Baerlocher, G. M., Vulto, I., Poon, S. S. & Lansdorp, P. M. Collapse of telomere homeostasis in hematopoietic cells caused by heterozygous mutations in telomerase genes. *PLoS Genet* **8**, e1002696 (2012).
13. Baerlocher, G. M., Vulto, I., de Jong, G. & Lansdorp, P. M. Flow cytometry and FISH to measure the average length of telomeres (flow FISH). *Nat. Protoc.* **1**, 2365–2376 (2006).
14. Codd, V. et al. Polygenic basis and biomedical consequences of telomere length variation. *Nat. Genet* **53**, 1425–1433 (2021).
15. Armanios, M. & Blackburn, E. H. The telomere syndromes. *Nat. Rev. Genet.* **13**, 693–704 (2012).
16. Telomeres Mendelian Randomization Collaboration et al. Association Between Telomere Length and Risk of Cancer and Non-Neoplastic Diseases: A Mendelian Randomization Study. *JAMA Oncol.* **3**, 636 (2017).
17. DeBoy, E. A. et al. Familial Clonal Hematopoiesis in a Long Telomere Syndrome. *N. Engl. J. Med.* **388**, 2422–2433 (2023).
18. Schmutz, I. et al. TINF2 is a haploinsufficient tumor suppressor that limits telomere length. *eLife* **9**, e61235 (2020).
19. Kim, W. et al. Cancer-associated POT1 mutations lead to telomere elongation without induction of a DNA damage response. *EMBO J.* **40**, e107346 (2021).
20. Henry, M.-L., Osborne, J. & Else, T. POT1 Tumor Predisposition. In GeneReviews® (eds.656 Adam, M. P. et al.) (University of Washington, Seattle, Seattle (WA), 1993).
21. Li, C. et al. Genome-wide Association Analysis in Humans Links Nucleotide Metabolism to Leukocyte Telomere Length. *Am. J. Hum. Genet.* **106**, 389–404 (2020).
22. Burren, O. S. et al. Genetic architecture of telomere length in 462,666 UK Biobank whole-genome sequences. *Nat. Genet* **56**, 1832–1840 (2024).
23. Tummala, H. et al. Germline thymidylate synthase deficiency impacts nucleotide metabolism and causes dyskeratosis congenita. *Am. J. Hum. Genet.* **109**, 1472–1483 (2022).
24. D'Aronco, G. et al. SAMHD1 restricts the deoxyguanosine triphosphate pool contributing to telomere stability in telomerase-positive cells. *FASEB J.* **37**, e22883 (2023).
25. Mannherz, W. & Agarwal, S. Thymidine nucleotide metabolism controls human telomere length. *Nat. Genet* **55**, 568–580 (2023).
26. Cristofari, G. & Lingner, J. Telomere length homeostasis requires that telomerase levels are limiting. *EMBO J.* **25**, 565–574 (2006).
27. Damm, K. et al. A highly selective telomerase inhibitor limiting human cancer cell proliferation. *EMBO J.* **20**, 6958–6968 (2001).
28. Snetselaar, R. et al. Short telomere length in IPF lung associates with fibrotic lesions and predicts survival. *PLoS One* **12**, e0189467 (2017).
29. Xin, Z.-T. et al. Functional characterization of natural telomerase mutations found in patients with hematologic disorders. *Blood* **109**, 524–532 (2007).
30. Boyraz, B., Bellomo, C. M., Fleming, M. D., Cutler, C. S. & Agarwal, S. A novel TERC CR4/CR5 domain mutation causes telomere disease via decreased TERT binding. *Blood* **128**, 2089–2092 (2016).
31. Maine, I. P., Chen, S. F. & Windle, B. Effect of dGTP concentration on human and CHO telomerase. *Biochemistry* **38**, 15325–15332 (1999).
32. Sun, D., Lopez-Guajardo, C. C., Quada, J., Hurley, L. H. & Von Hoff, D. D. Regulation of Catalytic Activity and Processivity of Human Telomerase. *Biochemistry* **38**, 4037–4044 (1999).
33. Chen, Y., Podlevsky, J. D., Logeswaran, D. & Chen, J. J.-L. A single nucleotide incorporation step limits human telomerase repeat addition activity. *EMBO J.* **37**, e97953 (2018).
34. Lewandowicz, A., Tyler, P. C., Evans, G. B., Furneaux, R. H. & Schramm, V. L. Achieving the Ultimate Physiological Goal in Transition State Analogue Inhibitors for Purine Nucleoside Phosphorylase. *J. Biol. Chem.* **278**, 31465–31468 (2003).
35. Kicska, G. A. et al. Immucillin H, a powerful transition-state analog inhibitor of purine nucleoside phosphorylase, selectively inhibits human T lymphocytes. *Proc. Natl Acad. Sci. USA* **98**, 4593–4598 (2001).
36. Osada, Y. et al. Hypouricemic effect of the novel xanthine oxidase inhibitor, TEI-6720, in rodents. *Eur. J. Pharmacol.* **241**, 183–188 (1993).
37. Diehl, F. F. et al. Nucleotide imbalance decouples cell growth from cell proliferation. *Nat. Cell Biol.* **24**, 1252–1264 (2022).
38. Poddar, S. et al. Development and preclinical pharmacology of a novel dCK inhibitor, DI-87. *Biochem Pharm.* **172**, 113742 (2020).
39. Sarup, J. C. & Fridland, A. Identification of purine deoxyribonucleoside kinases from human leukemia cells: substrate activation by purine and pyrimidine deoxyribonucleosides. *Biochemistry* **26**, 590–597 (1987).
40. Abt, E. R. et al. Purine nucleoside phosphorylase enables dual metabolic checkpoints that prevent T cell immunodeficiency and TLR7-associated autoimmunity. *J. Clin. Invest.* **132**, e160852 (2022).
41. Bohman, C. & Eriksson, S. Deoxycytidine kinase from human leukemic spleen: preparation and characteristics of homogeneous enzyme. *Biochemistry* **27**, 4258–4265 (1988).
42. Munch-Petersen, B., Piskur, J. & Søndergaard, L. Four Deoxynucleoside Kinase Activities from Drosophila melanogaster Are Contained within a Single Monomeric Enzyme, a New Multifunctional Deoxynucleoside Kinase *. *J. Biol. Chem.* **273**, 3926–3931 (1998).
43. Gupta, A. et al. Telomere length homeostasis responds to changes in intracellular dNTP pools. *Genetics* **193**, 1095–1105 (2013).
44. Nordlund, P. & Reichard, P. Ribonucleotide Reductases. *Annu. Rev. Biochem.* **75**, 681–706 (2006).
45. Knecht, W. et al. A few amino acid substitutions can convert deoxyribonucleoside kinase specificity from pyrimidines to purines. *EMBO J.* **21**, 1873–1880 (2002).
46. Munch-Petersen, B., Cloos, L., Tyrsted, G. & Eriksson, S. Diverging substrate specificity of pure human thymidine kinases 1 and 2 against antiviral dideoxynucleosides. *J. Biol. Chem.* **266**, 9032–9038 (1991).
47. Batiuk, T. D., Schnizlein-Bick, C., Plotkin, Z. & Dagher, P. C. Guanine nucleosides and Jurkat cell death: roles of ATP depletion and accumulation of deoxyribonucleotides. *Am. J. Physiol. Cell Physiol.* **281**, C1776–C1784 (2001).
48. Traut, T. W. Physiological concentrations of purines and pyrimidines. *Mol. Cell Biochem* **140**, 1–22 (1994).
49. Gustafson, E. A., Schinazi, R. F. & Fingeroth, J. D. Human Herpesvirus 8 Open Reading Frame 21 Is a Thymidine and Thymidylate Kinase of Narrow Substrate Specificity That Efficiently Phosphorylates Zidovudine but Not Ganciclovir. *J. Virol.* **74**, 684–692 (2000).
50. Bellon, M. & Nicot, C. Regulation of Telomerase and Telomeres: Human Tumor Viruses Take Control. *JNCI: J. Natl Cancer Inst.* **100**, 98–108 (2008).
51. Gandhi, V. et al. A proof-of-principle pharmacokinetic, pharmacodynamic, and clinical study with purine nucleoside phosphorylase inhibitor immucillin-H (BCX-1777, forodesine). *Blood* **106**, 4253–4260 (2005).
52. Al-Kali, A., Gandhi, V., Ayoubi, M., Keating, M. & Ravandi, F. Forodesine: review of preclinical and clinical data. *Future Oncol.* **6**, 1211–1217 (2010).

53. Schmidt, T. T. et al. High resolution long-read telomere sequencing reveals dynamic mechanisms in aging and cancer. *Nat. Commun.* **15**, 5149 (2024).
54. Tham, C.-Y. et al. High-throughput telomere length measurement at nucleotide resolution using the PacBio high fidelity sequencing platform. *Nat. Commun.* **14**, 281 (2023).
55. Sholes, S. L. et al. Chromosome-specific telomere lengths and the minimal functional telomere revealed by nanopore sequencing. *Genome Res*. gr.275868.121. https://doi.org/10.1101/gr.275868.121 (2021).
56. Huffman, K. E., Levene, S. D., Tesmer, V. M., Shay, J. W. & Wright, W. E. Telomere Shortening Is Proportional to the Size of the G-rich Telomeric 3′-Overhang*. *J. Biol. Chem.* **275**, 19719–19722 (2000).
57. Roake, C. M. & Artandi, S. E. Regulation of human telomerase in homeostasis and disease. *Nat. Rev. Mol. Cell Biol.* **21**, 384–397 (2020).
58. Wong, J. M. Y. & Collins, K. Telomerase RNA level limits telomere maintenance in X-linked dyskeratosis congenita. *Genes Dev.* **20**, 2848–2858 (2006).
59. Paulsen, B. S. et al. Ectopic expression of RAD52 and dn53BP1 improves homology-directed repair during CRISPR–Cas9 genome editing. *Nat. Biomed. Eng.* **1**, 878–888 (2017).
60. Agarwal, S. et al. Telomere elongation in induced pluripotent stem cells from dyskeratosis congenita patients. *Nature* **464**, 292–296 (2010).
61. Lai, T.-P., Wright, W. E. & Shay, J. W. Generation of digoxigenin-incorporated probes to enhance DNA detection sensitivity. *Biotechniques* **60**, 306–309 (2016).
62. Lyčka, M. et al. WALTER: an easy way to online evaluate telomere lengths from terminal restriction fragment analysis. *BMC Bioinforma.* **22**, 145 (2021).
63. Reilly, C. R. et al. The clinical and functional effects of TERT variants in myelodysplastic syndrome. *Blood* **138**, 898–911 (2021).

Acknowledgements

We thank the patients and families for research participation. We thank L. Homfeldt and J. Seo for technical assistance. We thank A. Gutierrez for suggesting the TRACE acronym. We thank A. Shimamura, M. Fleming and the BCH Bone Marrow Failure/ Myelodysplastic Syndrome Registry (National Institutes of Health (NIH) grant R21DK099808). This study was supported by: National Institutes of Health grants: F30DK135340 (W.M.), T32GM007753 (W.M.), T32GM144273 (W.M.), T32GM145407 (A.C.), R01DK107716 (S.A.), R33HL154133 (S.A.); Boston Children's Hospital Translational Research Program (S.A.); Harvard Stem Cell Institute (S.A.); Team Telomere (S.A.); Million Dollar Bike Ride/Penn Medicine Orphan Disease Center (S.A.); Philanthropic gifts (S.A.). This content is solely the responsibility of the authors and does not necessarily represent the official views of the National Institutes of Health.

Author contributions

S.A. and W.M. conceived of the study and designed experiments. W.M., A.C., and N.L. performed experiments. W.M. and A.C. analyzed the data and generated the figures. S.A. and W.M. wrote the paper with input and revisions from A.C. and N.L.

Competing interests

S.A. and W.M. are names as inventors on provisional patent applications relating to the data shown. The remaining authors declare no competing interests.

Additional information

Supplementary information The online version contains supplementary material available at https://doi.org/10.1038/s41467-025-58221-7.

Correspondence and requests for materials should be addressed to Suneet Agarwal.

Peer review information *Nature Communications* thanks Tracy Bryan, Jayakrishnan Nandakumar and the other, anonymous, reviewer(s) for their contribution to the peer review of this work. A peer review file is available.